

Adsorption of Azocarmine G dye on H₂SO₄-modified acacia sawdust

Celal Duran^{*1}, Sengul Tugba Ozeken^{1a}, Aslihan Yilmaz Camoglu^{1b} and Duygu Ozdes^{2c}

¹Karadeniz Technical University, Faculty of Sciences, Department of Chemistry, Trabzon, Turkey

²Gumushane University, Gumushane Vocational School, Gumushane, Turkey

(Received July 15, 2023, Revised March 2, 2024, Accepted March 14, 2024)

Abstract. Presence of hazardous dyes in water cause considerable risks to the human health and environment due to their potential toxicity and ecological disruptions. Therefore, in the present research, to suggest an alternative method for the retention of toxic Azocarmine G (ACG) dye from aqueous media, natural and H₂SO₄-modified acacia sawdust were performed for the first time as low-cost and efficient adsorbents. Based on batch experiments, it was determined that the best conditions for the developed dye retention process were an initial pH of 2.0 and an equilibrium time of 240 min. Analysis of the data using both pseudo-first order and pseudo-second order kinetic models showed that the retention of ACG onto the adsorbents predominantly occurred through chemical adsorption. Langmuir, Freundlich, and Dubinin-Radushkevich isotherm models were employed to provide insights into the interaction between the adsorbate and adsorbent and the mechanism of the adsorption process. Maximum monolayer adsorption capacities of natural and H₂SO₄-modified acacia sawdust were determined as 28.01 and 64.90 mg g⁻¹, respectively by Langmuir isotherm model. Results of the study clearly indicated that the modification of acacia sawdust with H₂SO₄ leads to a substantial increase in the adsorption performance of anionic dyes.

Keywords: acacia sawdust; adsorption; Azocarmine G; isotherm; kinetics; modification

1. Introduction

Dyes, while utilizing as colorants in several industries including leather, textiles, food, paper, and cosmetics, also raise concerns due to their potential toxic effects. The mitigating the adverse impression of dyes on living organisms and the environment have become crucial consideration (Gupta and Lataye 2017, Tounsadi *et al.* 2020, Naz *et al.* 2020, Khan *et al.* 2017). The toxic effects of azo dyes have gained significant attention due to their widespread use and potential hazards. Azo dyes, characterized by their azo (-N=N-) functional group, are commonly employed in numerous industries such as food, textiles, and plastics. Their complex molecular structure makes them difficult to break down through conventional degradation processes, leading to their persistence in the environment (Kuhad *et al.* 2004). Luan *et al.* (2017) reported that in some exceptional circumstances, azo dyes would activate changes in human DNA and cause lesions and induce cancer by decomposing into more than 20 kinds of aromatic amines, which are carcinogenic. Azocarmine G (ACG), a type of azo dyes, is commonly utilized in the food industry as a colorant and a biological stain for proteins and DNA (Khan *et al.* 2018). Current studies in the literature have primarily focused on the photo-degradation of ACG. However, it is worth noting that photo-degradation methods

often result in the formation of carcinogenic species that persist in aqueous media. This poses a challenge as these by-products require secondary treatment applications for their removal. Therefore, while photo-degradation shows promise as potential methods for ACG degradation, additional measures need to be taken to ensure the complete removal of harmful compounds. On the other hand, there are some studies about photo-catalytic degradation and mineralization of ACG (Luan *et al.* 2017), analyses of ACG concentration in food through high-performance liquid chromatography (Bonan *et al.* 2013), and preconcentration of ACG by cloud point extraction procedure with spectrophotometry (Khan *et al.* 2018).

A surface phenomenon called adsorption draws attention, in which an adsorbate is loaded onto an adsorbent through ion exchange, formation of chemical bonds, or interactions based on Van der Waals forces. Adsorption method is extensively utilized in industrial sectors for wastewater treatment technologies due to its numerous advantages, including being cost-effective, environmentally friendly, efficient, and easily applicable (Khan *et al.* 2016, Wang and Guo 2020, Topaloğlu and Yildirim 2021). Industrial sectors are increasingly interested in local abundant adsorbents due to their potential to reduce procurement and discharge costs in wastewater treatment processes. In recent years, there has been growing interest in utilizing large amounts of sawdust, which is a cost-effective and abundant adsorptive material, for the removal of various pollutants from wastewater. Sawdust, generated as an industrial by-product from wood processing, presents a dual advantage as it not only offers an effective solution for wastewater treatment but also helps address the disposal challenges associated with its abundance in everyday agricultural and industrial applications. Sawdust is an eco-

*Corresponding author, Ph.D., Professor,
E-mail: cduran@ktu.edu.tr

^a Ph.D.

^b Ph.D. Student

^c Professor

friendly material due to its carbon-rich content, porous surface morphology, large surface area, easy biodegradability, and chemical nature that can be easily modified (Meena *et al.* 2008, Yin *et al.* 2020, Mallakpour *et al.* 2021).

It has been reported that modifying the sawdust or other adsorbents enhance the adsorption capacity and lead to more efficient removal processes. By applying appropriate treatment methods, such as activation or functionalization, the adsorbent's surface properties can be modified, resulting in increased adsorption sites and improved interaction with the targeted pollutants. The treatment approach enhances the overall performance of the adsorbents and contributes to more effective uptake of contaminants during wastewater treatment. Silva *et al.* (2018) treated the acacia bark with organic solvents and inorganic acids and reported experiencing more efficient adsorption in crystal violet removal. Treated acacia sawdust was used for Pb(II), Cu(II), Hg(II), and Cr(VI) adsorption (Meena *et al.* 2008, Khalid *et al.* 2018). Activated carbon produced from acacia sawdust was used for the adsorptive removal of many dyes such as indigo carmine (Gupta and Lataye 2017), methyl orange (Danish *et al.* 2014), swiss blue (Jain *et al.* 2011), direct blue 2B (Nirmaladevi and Palanisamy 2019), methylene blue (Yusop *et al.* 2021, Tounsadi *et al.* 2020) and brilliant blue (Tounsadi *et al.* 2020). Acacia sawdust hydrochar and biochar were utilized in the uptake of basic red 29, reactive red 2, and acid blue 15 (Nirmaladevi and Palanisamy 2020, 2021).

In the present research natural and H₂SO₄-modified acacia sawdust were applied as adsorbents to remove ACG from aqueous media through batch adsorption method. While numerous research have evaluated the adsorptive removal of various anionic and cationic dyes using acacia sawdust, no studies about the adsorptive removal of ACG by natural or modified acacia sawdust have been noticed. The influences of initial solution pH, equilibrium time, initial ACG dye concentration and adsorbent amount were assessed on the adsorption performance of ACG for the optimization of the experimental conditions. The obtained results were applied to various isotherm and kinetic models to get an idea about the adsorption mechanism.

2. Materials and Methods

2.1 Chemicals and apparatus

Azocarmine G dye, NaOH, H₂SO₄, and HNO₃ were analytical grade, used without extra purification, and purchased from Fluka (Buch, Switzerland), or Merck (Darmstadt, Germany). ACG, also named Acid red 101, has the chemical formula of C₂₈H₁₈N₃NaO₆S₂ (579.6 g mol⁻¹). The calculated amount of ACG was weighed with Sartorius BP 1106 model analytical balance and dissolved in double distilled water to obtain a stock solution in 5.0 g L⁻¹ dye concentration. The stock dye solution was diluted with distilled water to prepare the standard and working solutions. The ACG level in the solution was analyzed by a Perkin Elmer Lambda 25 model UV-Vis spectrophotometer at a wavelength of 516 nm. The initial pH values of ACG

solutions were adjusted by diluted NaOH and HNO₃ solutions using the digital pH meter (Hanna pH-211). In batch adsorption experiments, Edmund Bühler GmbH model mechanical shaker model was utilized. Furthermore, for the separation of the adsorbent from the solutions, a Sigma 3-16P model centrifuge apparatus was employed. PerkinElmer 1600 Series Fourier Transform Infrared Spectrometer was used for determining the surface functional groups of natural-AS and H₂SO₄-AS. Scanning Electron Microscope (SEM) technique was utilized to assess the surface morphologies by ZEISS SIGMA 300.

2.2 Preparation of the adsorbent

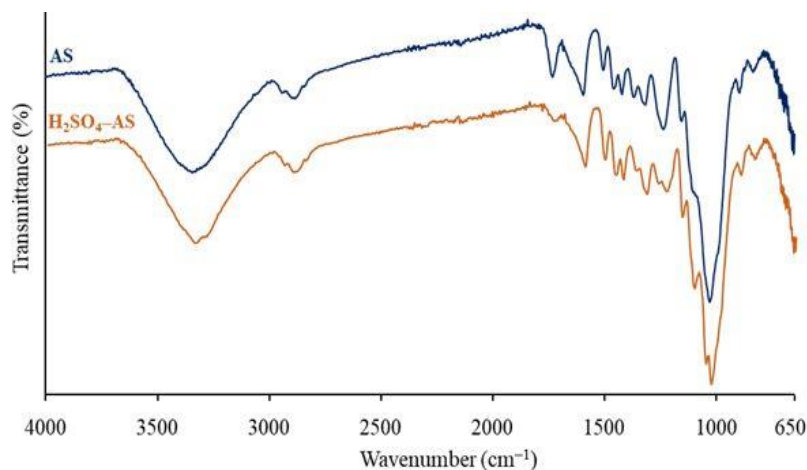
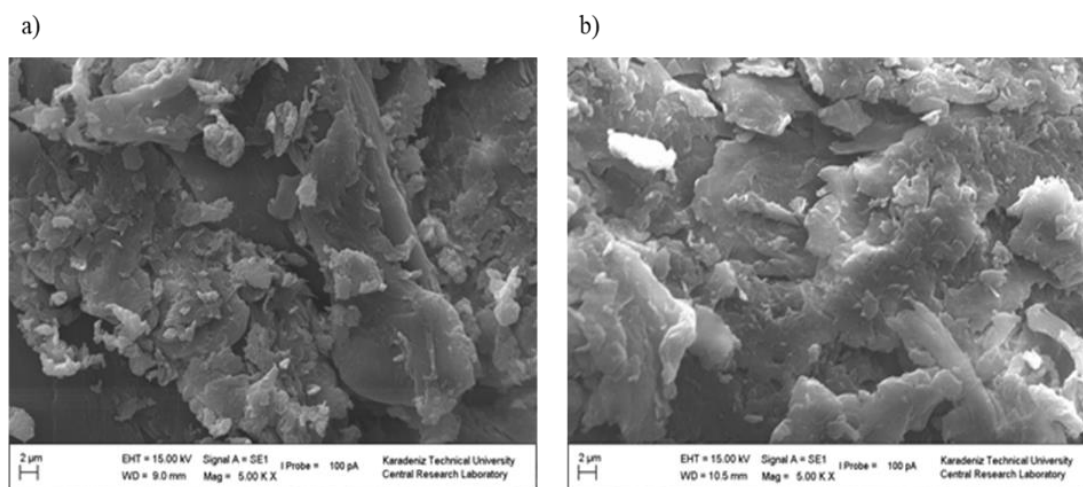
Acacia sawdust (AS), acquired from Gümüşhane (Türkiye) was ground by a blender. AS powder was sifted to separate the big particles, and only the particles smaller than 150 µm were stored in glass bottles for experimental studies. The modification was utilized by dipping 5.0 g of AS into 250 mL of 0.2 M H₂SO₄ solution and mixing the suspension by a magnetic stirrer at room temperature for 24 hours. Then the suspension was filtered through 0.45 µm pore-sized filter paper, and the solid sample was washed with distilled water up to when the pH of the filtrate reached to near neutral value. The modified adsorbent was dried in the oven at 80 °C for 12 hours (up to the constant weight), then kept in glass bottles. In other sections, natural acacia sawdust and H₂SO₄-modified acacia sawdust are named as AS and H₂SO₄-AS, respectively.

2.3 Batch adsorption experiments

The influences of the experimental variables on the adsorption efficiency of ACG onto H₂SO₄-AS were assessed through a batch method. All experiments were performed in triplicate. The procedure involved the following steps: I) Weighing the adsorbent; the adsorbent weighed using polypropylene centrifuge tubes. The weights ranged between 10 and 200 mg, II) Adding ACG solution; 10 mL of ACG solution with a pH value of 2.0 and concentrations ranging from 50 to 600 mg L⁻¹ were added to the tubes containing the adsorbents, III) Mixing; the mixtures of adsorbent and ACG solution were mechanically shaken at 400 rpm for various time intervals, ranging from 1 to 480 min. This ensured proper contact between the adsorbents and the ACG solution, IV) Centrifugation; after the predetermined time intervals, centrifugation was carried out at 3500 rpm for 5 min, V) Measurement of remaining ACG concentration; the level of ACG remaining in the solution was analyzed using a UV-Vis Spectrophotometer, VI) Calculation of uptaken ACG quantity; the amount of ACG adsorbed per gram of adsorbent (q_e) was calculated utilizing Eq. 1.

$$q_e = \frac{V(C_0 - C_e)}{m_s} \quad (1)$$

Initial and equilibrium concentration of ACG is given by C_0 (mg L⁻¹) and C_e (mg L⁻¹), respectively. V is the volume of the solution (L) and m_s is the adsorbent quantity (g).

Fig. 1 FTIR spectrum of AS and H₂SO₄-ASFig. 2 SEM images of a) AS and b) H₂SO₄-AS

3. Results and discussion

3.1 Characterization of AS and H₂SO₄-AS

The FTIR spectrum (Fig. 1), obtained by scanning the AS and H₂SO₄-AS in the interval of 4000–650 cm⁻¹, inform about the adsorptive functional groups of the adsorbents' surface. The broad bands with maximum values at 3332.8 cm⁻¹ (AS) and 3339.8 cm⁻¹ (H₂SO₄-AS) correspond to O-H stretching vibrations of hydroxyl groups (-OH) present in the main components (lignin, cellulose, and hemicellulose) of sawdust (Tounsadi *et al.* 2020). The peaks in the 2950–2850 cm⁻¹ interval for both AS materials may attribute to the stretching vibrations of C–H (aliphatic) (Nirmaladevi and Palanisamy 2021, Nirmaladevi and Palanisamy 2020). The peaks between 1200–1400 cm⁻¹ may be related with the stretching vibrations of C=O and C–H bonds in the present functional groups (aromatic groups, alcohols, and esters) (Nirmaladevi and Palanisamy 2021). The peaks seen at 1733, 1424, and 1026 cm⁻¹ may be due to C=O stretching (Ding *et al.* 2016, Serencam *et al.* 2014), CH₂ bending (Silva *et al.* 2018), and C–O–C function (Tounsadi *et al.* 2020), respectively. The band at 1505.5 cm⁻¹ may be related to the characteristic bands of lignin (Silva *et al.* 2018).

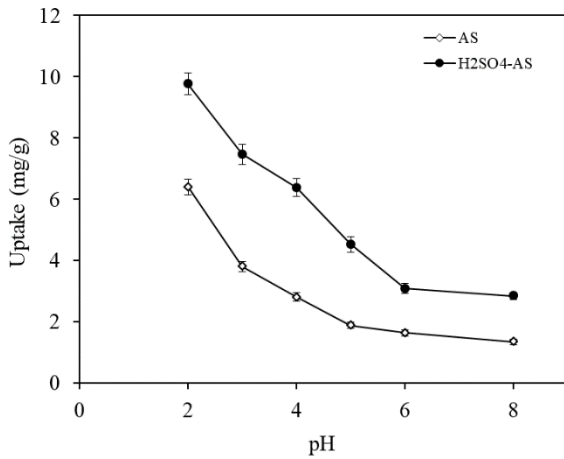
According to SEM images, it is noticed that the surface of AS is low porous and H₂SO₄ does not seem to have a significant effect on the morphological and chemical structure of the material (Fig. 2).

3.2 Optimizing of the initial pH

Adsorption performance is determined by the electrical charge carried by the adsorptive functional groups present on the surface of the adsorbent. These functional groups have a crucial contribution in attracting and binding the target molecules, thereby influencing the overall adsorption efficiency of an adsorbent. The electrical charge of an adsorbent is directly impacted by the pH of the solution. Therefore, in order to determine the most effective uptake of ACG, the effects of the initial solution pH was evaluated as the primary factor. For that purpose suspensions were prepared using either 5.0 g L⁻¹ of AS or H₂SO₄-AS. These suspensions were then contact with a solution containing 100 mg L⁻¹ of ACG within the pH range of 2.0 to 8.0. The H₂SO₄-AS demonstrated higher adsorption capacity than natural AS in all evaluated pH values (Fig. 3), indicating that modification has improved the adsorption efficiency. The observed effect is attributed to the use of sulfuric acid for the modification of the adsorbent. It is believed that the

Table 1 Kinetics parameters for ACG adsorption onto H₂SO₄-AS

$q_{e,exp}$ (mg g ⁻¹)	9.90 ± 0.28
PFO	
k_1 (min ⁻¹)	-0.0137
$q_{e,cal}$ (mg g ⁻¹)	5.29
R^2	0.9701
PSO	
k_2 (g mg ⁻¹ min ⁻¹)	0.0083
$q_{e,cal}$ (mg g ⁻¹)	10.14
R^2	0.9988
IPD	
$k_{id,1}$ (mg g ⁻¹ min ^{-1/2})	0.494
R^2	0.9619
$k_{id,2}$ (mg g ⁻¹ min ^{-1/2})	0.280
R^2	0.9511
C	4.50

Fig. 3 Initial pH effect on ACG adsorption (Equilibrium time: 240 min, Dye conc.: 100 mg L⁻¹, Adsorbent conc.: 5.0 g L⁻¹)

sulfuric acid treatment enlarges the pores of the adsorbent, which enhances its adsorption capacity. Additionally, the protonation of surface functional groups on the adsorbent's surface leads to better adsorption of the anionic ACG through electrostatic interactions. The uptake amount of ACG by both adsorbents decreased as the initial pH of the ACG solution increased in the 2.0-8.0 range. Maximum amounts of adsorbed ACG were observed at pH 2.0 and determined to be 6.40 ± 0.25 and 9.76 ± 0.35 mg per gram of AS and H₂SO₄-AS, respectively. The impacts of solution pH on ACG adsorption can be further explained by considering the pH_{pzc} (point of zero charge) value of the H₂SO₄-AS, which is determined to be 4.0. If the initial pH of the solution is adjusted to a lower pH than the determined value of pH_{pzc}, the functional groups on the adsorbent's surface charge positively (pH < pH_{pzc}). On the contrary, if the initial pH is higher than pH_{pzc}, these functional groups charged negatively (pH > pH_{pzc}) (Moharami

and Jalali 2013). In this study, the adsorption process necessitates an AS surface that is electrically positively charged to facilitate interactions between the adsorbent and the adsorbate. This is because ACG, being an anionic dye, requires an electrostatic attraction with the positively charged adsorbent surface for effective adsorption. As noticed in Fig. 3, the adsorption of ACG is higher at points where pH < pH_{pzc}. As the pH value approaches to the pH_{pzc} of the adsorbent, the uptake gradually decreases and at pH values higher than the pH_{pzc}, this decrease continues steadily. For the optimization of the subsequent experimental parameters, a pH value of 2.0 was selected.

3.3 Influences of contact time and kinetics of adsorption

To assess the appropriate equilibration time and minimize the retention time of ACG by H₂SO₄-AS, experiments were carried out for different contact times ranging from 1 to 480 min by using 100 mg L⁻¹ of initial ACG concentration at initial pH of 2.0 and 5.0 g L⁻¹ of H₂SO₄-AS. At the end of each determined time, the mixture of adsorbent and adsorbate was separated via centrifugation. The remaining ACG in the solution was then determined via UV-Vis Spectrometer. The adsorption process exhibited a gradual increase in uptake with increasing contact time. It was noticed that equilibrium was attained after 240 min, after which the uptake became nearly stable. This indicates that the adsorbent achieved its maximum uptake capacity for ACG and further contact time did not significantly affect the uptake (Fig. 4(a)).

The dominant controlling mechanisms were determined by applying pseudo-first order (PFO), pseudo-second order (PSO), and intraparticle diffusion (IPD) kinetic models to the experimental data. Linear equations of the PFO and PSO models are represented in Eq. 2 (Lagergren 1898) and Eq. 3 (Ho and McKay 1998), respectively.

$$\ln(q_e - q_t) = \ln q_e - k_1 t \quad (2)$$

$$\frac{t}{q_t} = \frac{1}{k_2 q_e^2} + \frac{t}{q_e} \quad (3)$$

q_t (mg g⁻¹) is the amount of ACG adsorbed onto 1 gram of H₂SO₄-AS at any time (t , min). $q_{e,cal}$ values are the amounts of ACG adsorbed per g of H₂SO₄-AS calculated by PFO and PSO kinetic models (mg g⁻¹), while $q_{e,exp}$ is the experimentally observed amount of ACG adsorbed onto 1 g of H₂SO₄-AS adsorbent (mg g⁻¹). k_1 (min⁻¹) and k_2 (g mg⁻¹ min⁻¹) are the rate constant of PFO and PSO kinetic models, respectively.

k_1 and $q_{e,cal}$ are the constants of the PFO model corresponding to the slope and the intercept of the linear plot of $\ln(q_e - q_t)$ versus t , while k_2 and the other $q_{e,cal}$ in Table 1 are the constants of the PSO model obtained from the intercept and slope of the plot of t/q_t versus t (Fig. 4(b)), respectively. $q_{e,cal}$ value was obtained to be 5.29 mg g⁻¹ for the PFO model by evaluating Eq. 2 and 10.14 mg g⁻¹ for the PSO model by evaluating Eq. 3 (Table 1). R^2 values of the PFO and PSO models were both higher than 0.9 and close to each other. On the other hand, the experimental ($q_{e,exp}$)

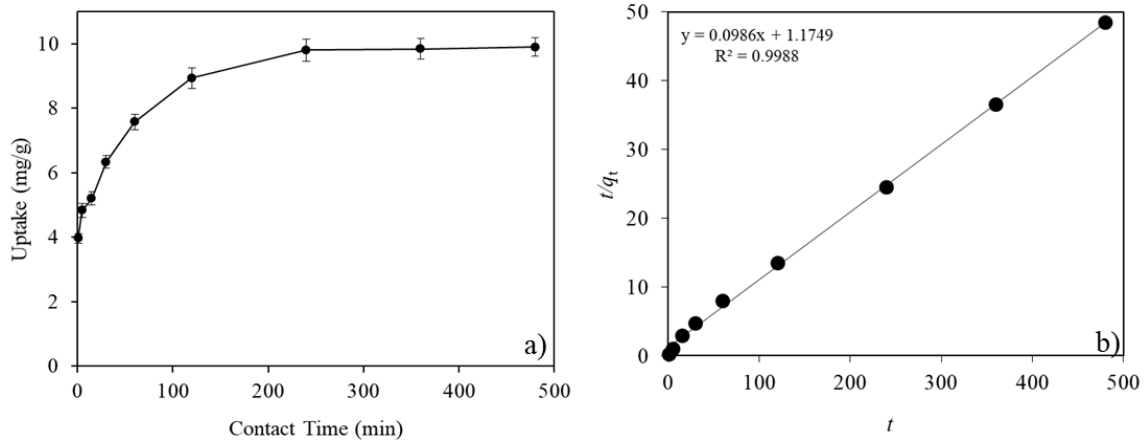


Fig. 4 a) Influences of equilibrium time on the retention of ACG by H₂SO₄ modified AS (Initial dye conc.: 100 mg L⁻¹, initial pH: 2.0, H₂SO₄-AS conc.: 5.0 g L⁻¹) b) Pseudo- second order kinetic model

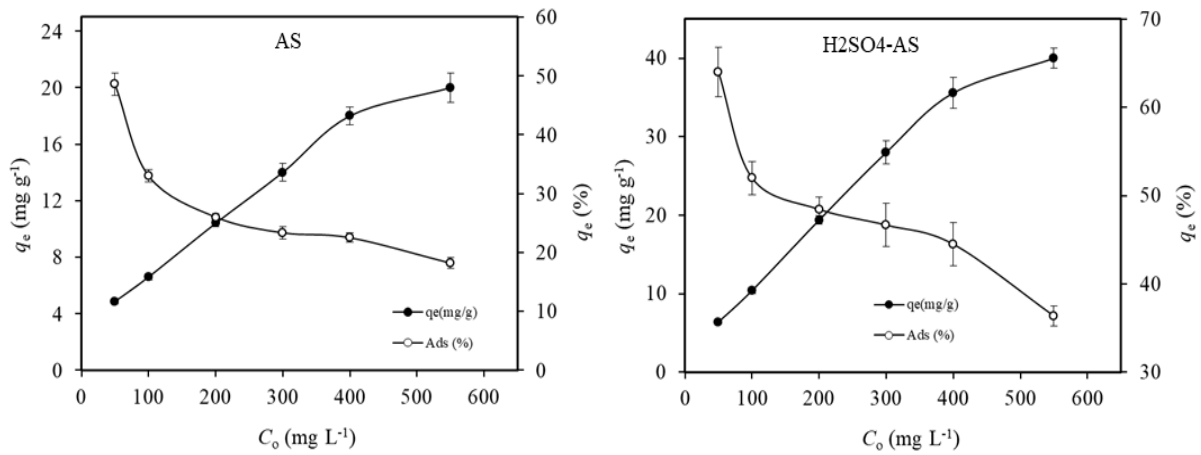


Fig. 5 Influences of initial ACG concentration on its uptake (adsorbent conc.: 5.0 g L⁻¹, initial pH: 2.0, contact time: 240 min)

and calculated ($q_{e,cal}$) values were compared for both models. The PSO model with a closer $q_{e,cal}$ value to $q_{e,exp}$, and a relatively higher R^2 value (0.9988) seems to fit very well for understanding the mechanism and describing the adsorption of ACG dye onto H₂SO₄-AS. This comparison supports the idea that chemisorption controlled the reaction rate of ACG adsorption onto H₂SO₄-AS. The chemical nature of adsorption means that the adsorbate molecules (ACG) bind to the adsorbent surface (H₂SO₄-AS) by forming chemical bonds. In this case, the interactions between the adsorbate and the adsorbent surface are chemical in nature, resulting in ionic interactions or other chemical bonding mechanisms. It is thought that functional groups such as C=O, -OH and C-O-C, etc. on the structure of the adsorbent are effective in this binding. As a confirmation of the same result, the color removal of ACG by the seeds of different plants was reported to follow the PSO model by Onukwuli and Obiora-Okafo (2019).

Eq. 4 expresses the IPD model (Weber and Morriss 1963).

$$q_t = k_{id}t^{1/2} + c \quad (4)$$

According to the IPD model, k_{id} (mg g⁻¹ min^{-1/2}) is the

rate constant, and C is a parameter that informs about the thickness of the boundary layer. In the IPD model, the adsorption process materializes in three steps according to a sighted multilinearity in the plot of q_t versus $t^{1/2}$ (figure not shown), which attribute to i) Film diffusion; ACG molecules in the bulk solution transport to the outer surface of the H₂SO₄-AS, ii) Intraparticle or pore diffusion; ACG molecules on the external surface are adsorbed into the pores of the H₂SO₄-AS gradually and inspect the adsorption rate, iii) Rapid adsorption; ACG molecules are rapidly adsorbed onto the active sites of the pores in the internal surface of H₂SO₄-AS.

If the plot of q_t versus $t_{1/2}$ passes through the origin, it demonstrates that the adsorption process is predominantly limited by pore diffusion alone. In this case, the rate at which adsorbate molecules diffuse through the pores of the adsorbent determines the overall reaction rate. However, if the plot of q_t versus $t_{1/2}$ does not pass through the origin, it suggests that both pore diffusion and film diffusion contribute to controlling the adsorption process. In such situations, the combined effects of pore diffusion (adsorbate diffusion through the internal pores) and film diffusion (mass transfer between the bulk solution and the external

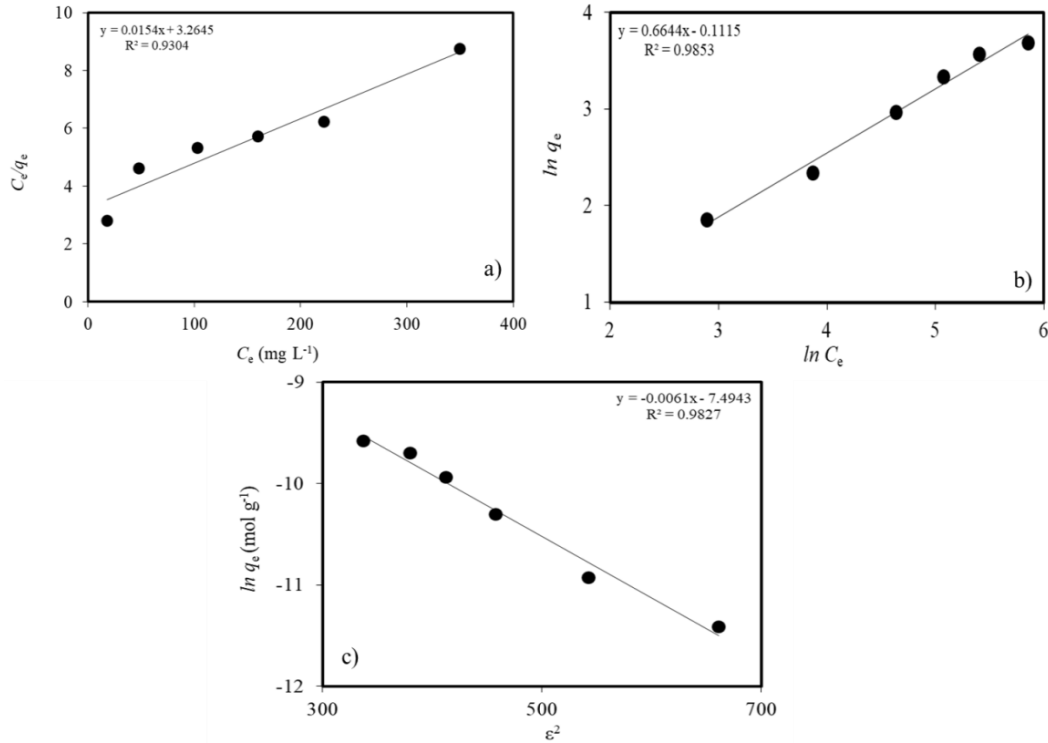


Fig. 6 a) Langmuir b) Freundlich c) Dubinin Radushkevich (D-R) isotherms for H₂SO₄-AS

surface of the adsorbent) are responsible for influencing the adsorption rate (Constantin *et al.* 2013, Wang *et al.* 2005, Hameed and El-Khaiary 2008). Detailed information about the mechanism of ACG adsorption onto H₂SO₄-AS is ensured by evaluating the C value and the rate constants ($k_{id,1}$ and $k_{id,2}$) of the IPD model. According to Table 1, $k_{id,2}$ (0.280 mg g⁻¹ min^{-1/2}) is lower than $k_{id,1}$ (0.494 mg g⁻¹ min^{-1/2}), indicating that the rate-limiting step is intra-particle diffusion in the ACG adsorption onto H₂SO₄-AS process. The intercept of q_t versus $t^{1/2}$ plot gave a C parameter that did not pass through the origin, which means that possibly intra-particle diffusion and surface film diffusion define the mechanism of ACG adsorption onto H₂SO₄-AS together.

3.4 Impact of initial ACG concentration

To examine the impact of the initial dye concentration on its uptake, different concentrations of ACG within the range of 50-550 mg L⁻¹ were tested. The data obtained experimentally illustrated that as the ACG concentration is increased in the 50-550 mg L⁻¹ range, the amount of ACG uptake by AS and H₂SO₄-AS increased from 4.86 ± 0.19 to 20.00 ± 1.06 mg g⁻¹, and from 6.40 ± 0.28 to 40.00 ± 1.28 mg g⁻¹, respectively. On the contrary, as the initial ACG concentration is increased in the same range, the adsorption percentages of ACG onto AS and H₂SO₄-AS decreased from 48.60 ± 1.90 to 18.18 ± 0.96 % and from 64.00 ± 2.82 to 36.36 ± 1.16 %, respectively (Fig. 5). The increase in the amount of ACG while keeping the adsorbent amount constant creates a driving force for mass transfer. As a result, the adsorbed dye amount per gram of adsorbent increases. Furthermore, it is important to note that

increasing the amount of ACG can lead to saturation of the adsorption surfaces. This can result in a lower adsorption percentage, as the remaining ACG molecules in the solution may not be able to bind to the fully occupied adsorption sites (Sharma *et al.* 2010, Lee *et al.* 2021).

Isotherm models were used to obtain descriptive information about the interactions between ACG dye and AS adsorbent at the equilibrium. Monolayer-like behavior of specific homogeneous sites, in which the interactions prevented between each other, is characteristic of the Langmuir model (Langmuir 1918). Conversely, the Freundlich model is characterized by multilayer adsorption, which occurs due to interactions between the adsorbed species on a heterogeneous surface. In this model, the available surface sites are energetically distinct from each other, leading to the formation of multiple layers of adsorbate molecules (Freundlich 1906). Extra knowledge about the type of adsorption is obtained by evaluating the D-R model (Dubinin and Radushkevich 1947).

The linearized form of the Langmuir and Freundlich models are given by Eq.5 and Eq. 6, respectively:

$$\frac{C_e}{q_e} = \frac{C_e}{q_{\max}} + \frac{1}{bq_{\max}} \quad (5)$$

$$\ln q_e = \ln K_f + \frac{1}{n} \ln C_e \quad (6)$$

C_e (mg L⁻¹); equilibrium ACG concentration in solution, q_e (mg g⁻¹); amount of ACG retention, q_{\max} (mg g⁻¹); maximum monolayer adsorption capacity, b (L mg⁻¹); free energy of the adsorption, n ; adsorption density, K_f (mg g⁻¹); adsorption capacity, n ; a unitless constant representing the adsorption density.

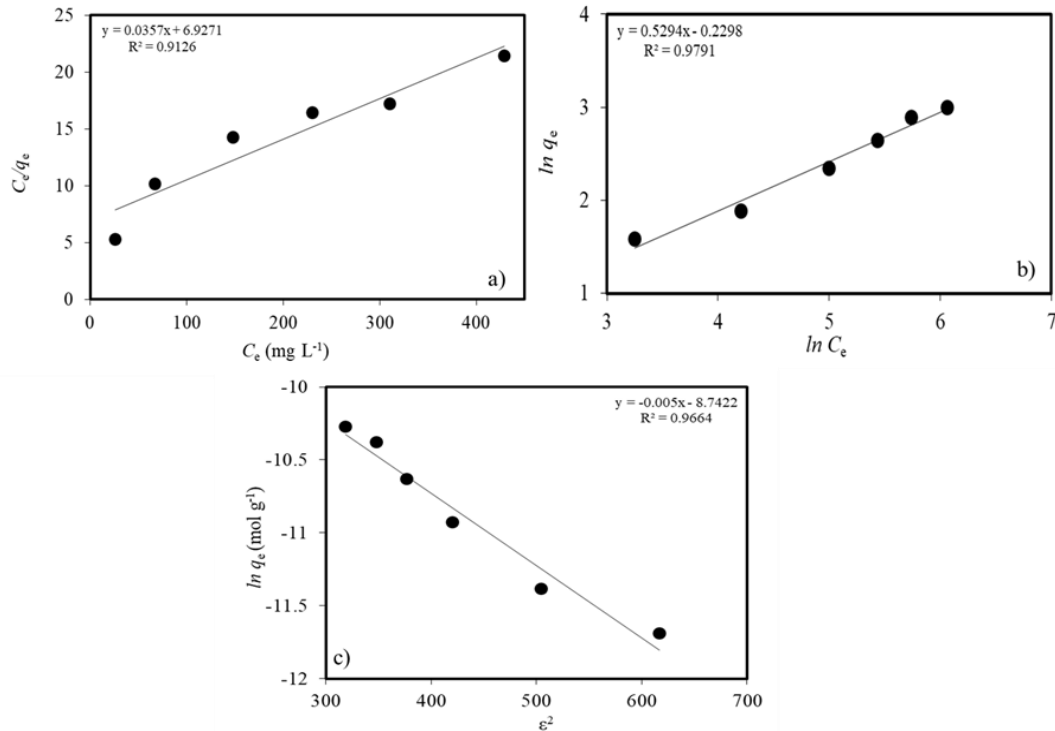


Fig. 7 a) Langmuir b) Freundlich c) Dubinin Radushkevich (D-R) isotherms for AS

R_L is a dimensionless equilibrium parameter (Langmuir separation factor) calculated from Eq. 7 (Hall *et al.* 1966), which gives a chance to interpret the favorability of adsorption.

$$R = \frac{1}{1+b.C_0} \quad (7)$$

R_L is zero in an irreversible process, yet, $0 < R_L < 1$ is the clue of suitable adsorption. $R_L = 1$ points out a linear case, and $R_L > 1$ points out that the occurring process is unfavorable at the equilibrium.

Figs. 6 and 7 illustrate the isotherm models for H₂SO₄-modified AS and AS, respectively. By evaluating Eq. 5, b and q_{max} are determined by the intercept and the slope of C_e/q_e versus C_e plot, respectively. The maximum adsorption capacities of AS and H₂SO₄-AS were 28.01 mg g⁻¹ and 64.90 mg g⁻¹, respectively which reveals an improved adsorption owing to the modification process. Sulfuric acid treatment may expand the pores of the AS, thereby increasing its adsorption capacity. Moreover, the protonation of surface functional groups on the AS enhances the adsorption of the anionic ACG through improved electrostatic interactions. The proposed adsorbents demonstrate a superior adsorption capacity compared to many acacia-based sawdust materials and some other types of adsorbents listed in Table 3, which are often difficult to prepare and costly (Zhang *et al.* 2017, Nirmaladevi and Palanisamy 2019, 2020 and 2021, Hanafiah *et al.* 2012, Tounsadi *et al.* 2020, Constantin *et al.* 2013, Terangpi and Chakraborty 2017, Moussavi and Mahmoudi 2009, Rahman *et al.* 2021, Doltabadi *et al.* 2016). The high adsorption capacity of the proposed adsorbents makes them highly competitive and desirable for various applications. R_L values determined in the range of

0.243-0.794 for AS and in the range of 0.262-0.810 for H₂SO₄-AS indicate that ACG adsorption onto natural and H₂SO₄-modified AS was favorable. According to Freundlich isotherm model, in order to calculate the K_f and n values, $\ln q_e$ versus $\ln C_e$ graph is plotted by evaluating Eq. 6 and the constants n and K_f are determined from the slope and intercept of this graph, respectively. The suitability of the developed process can be inferred from the range of the constant ' n ' in the Freundlich model, which typically falls between 1 and 10. This value signifies the intensity of adsorption and supports the favorable nature of the adsorption process. The fact that the constant ' n ' falls between 1 and 10 suggests that the developed process is well-suited for efficient adsorption of the target species. In the present study n values were 1.89 for AS and 1.51 for H₂SO₄-AS which demonstrates the favorability of ACG adsorption onto both adsorbents. The calculated correlation coefficients (R^2) evaluated by the equations of Freundlich and Langmuir models were compared. Higher R^2 values were obtained from the Freundlich model, indicating that the active sites on AS and H₂SO₄-AS surfaces were distributed heterogeneously and allowed multilayer adsorption of ACG (Table 2).

Eq. 8 is the linearized form of the D-R model and provides more information about the ACG's adsorption mechanism through the calculations of Polanyi potential (ϵ) using Eq. 9 and the mean adsorption energy (E , kJ mol⁻¹) using Eq. 10.

$$\ln q_e = \ln q_m - \beta \epsilon^2 \quad (8)$$

$$\epsilon = RT \ln(1 + 1/C_e) \quad (9)$$

Table 2 Langmuir, Freundlich, and Dubinin Radushkevich (D-R) isotherm parameters for the adsorption of ACG

		Natural-AS	H ₂ SO ₄ -AS
Langmuir isotherm model	q_{\max} (mg g ⁻¹)	28.01	64.90
	b (L mg ⁻¹)	0.0052	0.0047
	R^2	0.9126	0.9304
Freundlich isotherm model	K_f (mg g ⁻¹)	0.795	0.894
	n	1.89	1.51
	R^2	0.9791	0.9853
D-R isotherm model	q_m (mg g ⁻¹)	9.62	17.96
	β (kJ ² mol ⁻²)	-0.0050	-0.0061
	E (kJ mol ⁻¹)	10.00	9.05
	R^2	0.9664	0.9827

Table 3 Comparison of the maximum dye adsorption capacities of various adsorbents

Adsorbent	Anionic dye	q_{\max} (mg g ⁻¹)	Reference
Gemini 12-2-12 surfactant-modified wheat bran	Acid Red 18	60.75	Zhang <i>et al.</i> 2017
	Acid Orange 7	85.12	
	Acid Black 1	79.12	
Acacia sawdust biochar	Reactive Red 2	232	Nirmaladevi and Palanisamy 2020
Activated carbon from ZnCl ₂ activated acacia wood sawdust hydrochar	Direct Blue 2B	37	Nirmaladevi and Palanisamy 2019
	<i>Shorea dasphylla</i> sawdust	Acid Blue 25	Hanafiah <i>et al.</i> 2012
Biochar prepared from AS	Acid Blue 15	40.88	Nirmaladevi and Palanisamy 2021
ZnCl ₂ activated hydrochar prepared from AS		84.43	
NaOH treated acacia sawdust	Brilliant Blue	8.13	Tounsadi <i>et al.</i> 2020
HCl treated acacia sawdust		6.19	
Crosslinked poly (acrylamidopropyl trimethylammonium) grafted pullulan	Azocarmine B	113.6	Constantin <i>et al.</i> 2013
Amine based polymer aniline formaldehyde condensate	Acid orange 8	164	Terangpi and Chakraborty 2017
	Acid violet 7	68	
MgO nanoparticles	Remozal brilliant Blue R	166.7	Moussavi and Mahmoudi 2009
	Reactive red 198	123.5	
<i>Ailanthus altissima</i> sawdust	Acid Yellow 29	9.464	Rahman <i>et al.</i> 2021
Sawdust-Based Adsorbent (HCl treated)	Reactive Red 196	13.39	Doltabadi <i>et al.</i> 2016
	AS	28.01	
H ₂ SO ₄ -modified AS	Azocarmine G	64.90	<i>This Study</i>

$$E = 1/(-2\beta)^{1/2} \quad (10)$$

q_m (mg g⁻¹) is the adsorption capacity and β (kJ² mol⁻²) is the activity coefficient. q_m and β are the constants of the D-R model which can be calculated by the intercept and the slope of the linear plot of $\ln q_e$ versus ε^2 , respectively. The adsorption energy, E , provides idea about the mechanism of adsorption in three separate circumstances. Firstly, if the calculated E value is higher than 16 kJ mol⁻¹, it indicates the possibility of chemical adsorption. Hence, the adsorption process involves chemical interactions between the adsorbent and the adsorbate. Secondly, if the E value is in the range of 8-16 kJ mol⁻¹, it refers an adsorption mechanism based on ion exchange. Lastly, if the E value is smaller than 8 kJ mol⁻¹, it indicates a physical adsorption mechanism including van der Waals forces or dipole-dipole interactions (Helfferich 1962, Lee *et al.* 2021). E values were calculated as 10.00 and 9.05 kJ mol⁻¹ for ACG adsorption onto AS and H₂SO₄-modified AS, respectively, showing that these

processes occur chemically through an ion-exchange mechanism in nature.

3.5 Impact of the amount of H₂SO₄-AS

To reveal the influences of adsorbent amount on its performance in ACG uptake process, various H₂SO₄-AS dosages ranging between 1.0 and 20.0 g L⁻¹ were evaluated. The amount of adsorbed ACG per g of H₂SO₄-AS at the equilibrium and the removal efficiencies (%) of ACG were plotted against the concentration of modified adsorbent (Fig. 8). The adsorption amount of ACG decreased from 108.1 ± 5.1 to 10.6 ± 0.7 mg g⁻¹ as the adsorbent dosage was increased in the 1.0-20.0 g L⁻¹ range, possibly because of overlapping or aggregation of the active adsorptive sites on the adsorbent surface (Crini *et al.* 2007). When the quantity of H₂SO₄-AS was increased in the same range, the uptake percentage of ACG increased from 43.2 ± 2.0 to 84.8 ± 1.6 % a result of the increased number of solid

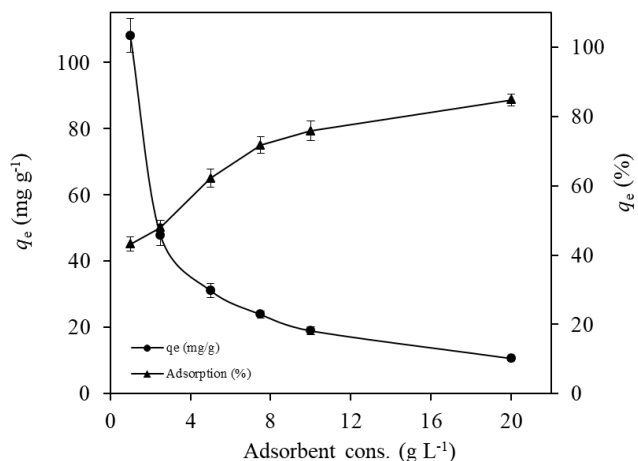


Fig. 8 Effect of H₂SO₄-AS amount on ACG adsorption (Initial dye conc.: 250 mg L⁻¹, initial pH: 2.0, contact time: 240 min)

particles containing higher numbers of adsorptive sites (Crini *et al.* 2007).

4. Conclusions

The adsorptive removal of hazardous Azocarmine G dye by natural and sulfuric acid-modified acacia sawdust was evaluated for the first time. The present research has gained important attention from both environmental and industrial viewpoint due to the requirement for low cost and easily available materials to effectively remove the harmful dyes from wastewater prior to its discharge. The study investigated the impacts of different experimental factors on the adsorption efficiency of ACG dye. Through the evaluation of the obtained data, the optimum pH for ACG adsorption was specified to be 2.0. Additionally, it was noticed that the uptake efficiency of ACG reached maximum value at an equilibrium time of 240 min. Furthermore, H₂SO₄-AS exhibited a higher dye adsorption capacity compared to many other adsorbents mentioned in the literature. This highlights the effectiveness of the modification process in enhancing the adsorption performance of the adsorbents and demonstrates their potential as superior materials for dye removal. Overall, the importance of the research stems from its potential to meet the demand for cost-effective and abundant materials to efficiently remove harmful dyes from wastewater, thereby protecting the environment and human health.

References

Bonan, S., Fedrizzi, G., Menotta, S. and Elisabetta, C. (2013), "Simultaneous determination of synthetic dyes in foodstuffs and beverages by high-performance liquid chromatography coupled with diode-array detector", *Dyes Pigments*, **99**(1), 36-40. <https://doi.org/10.1016/j.dyepig.2013.03.029>

Constantin, M., Asmarandei, I., Harabagiu, V., Ghimici, L., Ascenzi, P. and Fundueanu, G. (2013), "Removal of anionic dyes from aqueous solutions by an ion-exchanger based on

pullulan microspheres", *Carbohydr. Polym.*, **91**(1), 74-84. <https://doi.org/10.1016/j.carbpol.2012.08.005>

Crini, G., Peindy, H.N., Gimbert, F. and Robert, C. (2007), "Removal of C.I. Basic Green 4 (Malachite Green) from aqueous solutions by adsorption using cyclodextrin-based adsorbent: Kinetic and equilibrium studies", *Sep. Purif. Technol.*, **53**(1), 97-110. <https://doi.org/10.1016/j.seppur.2006.06.018>

Danish, M., Hashim, R., Mohamad Ibrahim, M.N. and Sulaiman, O. (2014), "Response surface methodology approach for methyl orange dye removal using optimized *Acacia mangium* wood activated carbon", *Wood Sci. Technol.*, **48**, 1085-1105. <https://doi.org/10.1007/s00226-014-0659-7>

Ding, R., Wu, H., Thunga, M., Bowler, N. and Kessler, M.R. (2016), "Processing and characterization of low-cost electrospun carbon fibers from organosolv lignin/polyacrylonitrile blends", *Carbon*, **100**, 126-136. <https://doi.org/10.1016/j.carbon.2015.12.078>

Doltabadi, M., Alidadi, H. and Davoudi, M. (2016), "Comparative study of cationic and anionic dye removal from aqueous solutions using sawdust-based adsorbent", *Environ. Prog. Sustain. Energy*, **35**(4), 1078-1090. <https://doi.org/10.1002/ep.12334>

Dubinin, M.M. and Radushkevich, L.V. (1947), "Equation of the characteristic curve of activated charcoal", *Proceedings of the Academy of Sciences of the USSR, Physical Chemistry Section*, **55**, 331-333.

Freundlich, H.M.F. (1906), "Über die adsorption in Lösungen", *Z. Phys. Chem.*, **57**, 385-470.

Gupta, T.B. and Lataye, D.H. (2017), "Adsorption of indigo carmine dye onto *acacia nilotica* (babool) sawdust activated carbon", *J. Hazard. Toxicol. Radioact. Waste*, **21**(4), 1-11. [https://doi.org/10.1061/\(ASCE\)HZ.2153-5515.0000365](https://doi.org/10.1061/(ASCE)HZ.2153-5515.0000365)

Hall, K.R., Eagleton, L.C., Acrivos, A. and Vermeulen, T. (1966), "Pore and solid diffusion kinetics in fixed bed adsorption under constant pattern conditions", *Ind. Eng. Chem. Fund.*, **5**(2), 212-223. <http://doi.org/10.1021/i160018a011>

Hameed, B.H. and El-Khaiary, M.I. (2008), "Kinetics and equilibrium studies of malachite green adsorption on rice straw-derived char", *J. Hazard. Mater.*, **153**(1-2), 701-708. <https://doi.org/10.1016/j.jhazmat.2007.09.019>

Hanafiah, M.A.K.M., Ngah, W.S.W., Zolkafly, S.H., Teong, L.C. and Majid, Z.A.A. (2012), "Acid Blue 25 adsorption on base treated *Shorea dasyphylla* sawdust: Kinetic, isotherm, thermodynamic and spectroscopic analysis", *J. Environ. Sci.*, **24**(2), 261-268. [https://doi.org/10.1016/S1001-0742\(11\)60764-X](https://doi.org/10.1016/S1001-0742(11)60764-X)

Helfferich, F. (1962), *Ion Exchange*, McGraw-Hill, New York.

Ho, Y.S. and McKay G. (1998), "Kinetic models for the sorption of dye from aqueous solution by wood", *Process Safe. Environ. Prot.*, **76**(2), 183-191.

Jain, M., Mudhoo, A. and Garg, V.K. (2011), "Swiss blue dye sequestration by adsorption using *Acacia nilotica* sawdust", *Int. J. Environ. Technol. Manag.*, **14**(1), 220-237.

Khalid, R., Aslam, Z., Abbas, A., Ahmad, W., Ramzan, N. and Shawabkeh, R. (2018), "Adsorptive potential of *Acacia Nilotica* based adsorbent for Chromium (VI) from an aqueous phase", *Chin. J. Chem. Eng.*, **26**(3), 614-622. <https://doi.org/10.1016/j.cjche.2017.08.017>

Khan, S.A., Shyamala, P., Kumar, K.R. and Suneetha, D. (2018), "Development of new cloud point extraction procedure using mixed micelles of TX-114 and DOSS for the determination of azocarmine G", *J. Indian Chem. Soc.*, **95**, 1085-1088.

Khan, M.A., Khan, M.I. and Zafar, S. (2017), "Removal of different anionic dyes from aqueous solution by anion exchange membrane", *Membr. Water Treat.*, **8**(3), 259-277. <https://doi.org/10.12989/mwt.2017.8.3.259>

- Khan, M.I., Wu, L., Mondal, A.N., Yao, Z., Ge, L. and Xu, T. (2016), "Adsorption of methyl orange from aqueous solution on anion exchange membranes: Adsorption kinetics and equilibrium", *Membr. Water Treat.*, **7**(1), 23-38. <http://doi.org/10.12989/mwt.2016.7.1.023>
- Kuhad, R.C., Sood, N., Tripathi, K.K., Singh, A. and Ward, O.P. (2004), "Developments in microbial methods for the treatment of dye effluents", *Adv. Appl. Microbiol.*, **56**, 185-213. [http://doi.org/10.1016/S0065-2164\(04\)56006-9](http://doi.org/10.1016/S0065-2164(04)56006-9)
- Lagergren, S. (1898), "About the theory of so-called adsorption of soluble substance", *Kungl. Svenska Vetenskapskad. Handl.*, **24**, 1-39.
- Langmuir, I. (1918), "The adsorption of gases on plane surfaces of glass, mica and platinum", *J. Am. Chem. Soc.*, **40**(9), 1361-1403.
- Lee, X.J., Hiew, B.Y.Z., Lai, K.C., Tee, W.T., Thangalazhy-Gopakumar, S., Gan, S. and Lee, L.Y. (2021), "Applicability of a novel and highly effective adsorbent derived from industrial palm oil mill sludge for copper sequestration: Central composite design optimisation and adsorption performance evaluation", *J. Environ. Chem. Eng.*, **9**(5), 105968. <https://doi.org/10.1016/j.jece.2021.105968>
- Luan, J., Shen, Y., Wang, S. and Guo, N. (2017), "Synthesis, property characterization and photocatalytic activity of the Polyaniline/BiYTi₂O₇ polymer composite", *Polymers*, **9**(3), 69. <https://doi.org/10.3390/polym9030069>
- Mallakpour, S., Sirous, F. and Hussain, C.M. (2021), "Sawdust, a versatile, inexpensive, readily available bio-waste: From mother earth to valuable materials for sustainable remediation Technologies", *Adv. Colloid Interf. Sci.*, **295**, 102492. <https://doi.org/10.1016/j.cis.2021.102492>
- Meena, A.K., Kadirvelu, K., Mishra, G.K., Rajagopal, C. and Nagar, P.N. (2008), "Adsorptive removal of heavy metals from aqueous solution by treated sawdust (*Acacia arabica*)", *J. Hazard. Mater.*, **150**(3), 604-611. <https://doi.org/10.1016/j.jhazmat.2007.05.030>
- Moharami, S. and Jalali, M. (2013), "Removal of phosphorus from aqueous solution by Iranian natural adsorbents", *Chem. Eng. J.*, **223**, 328-339. <https://doi.org/10.1016/j.cej.2013.02.114>
- Moussavi, G. and Mahmoudi, M. (2009), "Removal of azo and anthraquinone reactive dyes from industrial wastewaters using MgO nanoparticles", *J. Hazard. Mater.*, **168**(2-3), 806-812. <https://doi.org/10.1016/j.jhazmat.2009.02.097>
- Naz, A., Masood, H., Ehsan, S. and Tahir, T. (2020), "Removal of acid black 1 by *Acacia Concinna*; adsorption kinetics, isotherm and thermodynamic study", *Membr. Water Treat.*, **11**(6), 407-416. <https://doi.org/10.12989/mwt.2020.11.6.407>
- Nirmaladevi, S. and Palanisamy, N. (2020), "A comparative study of the removal of cationic and anionic dyes from aqueous solutions using biochar as an adsorbent", *Desalin. Water Treat.*, **175**, 282-292. <https://doi.org/10.5004/dwt.2020.24906>
- Nirmaladevi, S. and Palanisamy, N. (2019), "Preparation and adsorptive properties of activated carbon from *acacia leucophloea* wood sawdust hydrochar by zinc chloride activation", *Cellul. Chem. Technol.*, **53**(9-10), 1029-1039. <https://doi.org/10.35812/CelluloseChemTechnol.2019.53.101>
- Nirmaladevi, S. and Palanisamy, P.N. (2021), "Adsorptive behavior of biochar and zinc chloride activated hydrochar prepared from *Acacia leucophloea* wood sawdust: kinetic equilibrium and thermodynamic studies", *Desalin. Water Treat.*, **209**, 170-181. <https://doi.org/10.5004/dwt.2021.26515>
- Onukwuli, O.D. and Obiora-Okafo, I.A. (2019), "Performance of polymer coagulants for colour removal from dye simulated medium: Polymer adsorption studies", *Indian J. Chem. Technol.*, **26**, 205-215. <https://doi.org/10.56042/ijct.v26i3.14840>
- Rahman, N., Ullah, I., Alam, S., Khan, M.S., Shah, L.A., Zekker, I., Burlakovs, J., Kallistova, A., Pimenov, N., Vincevica-Gaile, Z., Jani, Y. and Zahoor, M. (2021), "Activated *Ailanthus altissima* sawdust as adsorbent for removal of acid yellow 29 from wastewater: Kinetics approach", *Water*, **13**, 2136. <https://doi.org/10.3390/w13152136>
- Serencam, H., Ozdes, D., Duran, C. and Senturk, H.B. (2014), "Assessment of kinetics, thermodynamics, and equilibrium parameters of Cu(II) adsorption onto *Rosa canina* seeds", *Desalin. Water Treat.*, **52**, 3226-3236. <https://doi.org/10.1080/19443994.2013.797377>
- Sharma, P., Kaur, R., Baskar, C. and Chung, W.J. (2010), "Removal of methylene blue from aqueous waste using rice husk and rice husk ash", *Desalination*, **259**(1-3), 249-257. <https://doi.org/10.1016/j.desal.2010.03.044>
- Silva, J.S., Rosa, M.P., Beck, P.H., Peres, E.C., Dotto, G.L., Kessler, F. and Grasel, F.S. (2018), "Preparation of an alternative adsorbent from *Acacia Mearnsii* wastes through acetosolv method and its application for dye removal", *J. Clean. Prod.*, **180**, 386-394. <https://doi.org/10.1016/j.jclepro.2018.01.201>
- Terangpi, P. and Chakraborty, S. (2017), "Adsorption kinetics and equilibrium studies for removal of acid azo dyes by aniline formaldehyde condensate", *Appl. Water Sci.*, **7**, 3661-3671. <https://doi.org/10.1007/s13201-016-0510-4>
- Topaloğlu, A.K. and Yildirim, Y. (2021), "Removal of reactive black 5 dye by using polyoxometalate-membrane", *Membr. Water Treat.*, **12** (1), 23-35. <https://doi.org/10.12989/mwt.2021.12.1.023>
- Tounsadi, H., Metarfi, Y., Barka, N., Taleb, M. and Rais, Z. (2020), "Removal of textile dyes by chemically treated sawdust of acacia: Kinetic and equilibrium studies", *J. Chem.* **2020**, 7234218. <https://doi.org/10.1155/2020/7234218>
- Wang, J. and Guo, X. (2020), "Adsorption isotherm models: Classification, physical meaning, application and solving method", *Chemosphere*, **258**, 127279. <https://doi.org/10.1016/j.chemosphere.2020.127279>
- Wang, S., Li, L., Wu, H. and Zhu, Z.H. (2005), "Unburned carbon as a low-cost adsorbent for treatment of methylene blue-containing wastewater", *J. Colloid Interf. Sci.*, **292** (2), 336-343. <https://doi.org/10.1016/j.jcis.2005.06.014>
- Weber, W.J. and Morris, J.C. (1963), "Kinetics of adsorption on carbon from solution", *J. Sanitary Eng. Division*, **89**, 31-60.
- Yin, Z., Li, Y., Song, T., Bao, M., Li, Y., Lu, J. and Li., Y. (2020), "Preparation of superhydrophobic magnetic sawdust for effective oil/water separation", *J. Clean. Prod.*, **253**, 120058. <https://doi.org/10.1016/j.jclepro.2020.120058>
- Yusop, M.F.M., Ahmad, M.A., Rosli, N.A. and Manaf, M.A.A. (2021), "Adsorption of cationic methylene blue dye using microwave-assisted activated carbon derived from acacia wood: Optimization and batch studies", *Arab. J. Chem.*, **14**(6), 103122. <https://doi.org/10.1016/j.arabjc.2021.103122>
- Zhang, Y., Huang, G., An, C., Xin, X., Liu, X., Raman, M., Yao, Y., Wang, W. and Doble, M. (2017), "Transport of anionic azo dyes from aqueous solution to gemini surfactant-modified wheat bran: Synchrotron infrared, molecular interaction and adsorption studies", *Sci. Total Environ.*, **595**, 723-732. <https://doi.org/10.1016/j.scitotenv.2017.04.031>